Friction **5**(1): 87–98 (2017)
DOI 10.1007/s40544-017-0140-3
ISSN 2223-7690
CN 10-1237/TH
RESEARCH ARTICLE

Influence of surgical suture properties on the tribological interactions with artificial skin by a capstan experiment approach

Gangqiang ZHANG[1,2,3], Tianhui REN[3], Xiangqiong ZENG[1,2,*], Emile VAN DER HEIDE[2,4]

[1] *Advanced Lubricating Materials Laboratory, Shanghai Advanced Research Institute, Chinese Academy of Sciences, Shanghai 201210, China*

[2] *Laboratory for Surface Technology and Tribology, University of Twente, Enschede 7500AE, the Netherlands*

[3] *School of Chemistry and Chemical Engineering, Key Laboratory for Thin Film and Microfabrication of the Ministry of Education, Shanghai Jiao Tong University, Shanghai 200240, China*

[4] *TU Delft, Faculty of Civil Engineering and Geosciences, Stevinweg 1, Delft 2628 CN, the Netherlands*

Received: 08 August 2016 / Revised: 26 October 2016 / Accepted: 11 December 2016

Abstract: Tribological interactions between surgical suture and human tissue play an important role in the stitching process. The purpose of the paper is to understanding the tribological behavior of surgical suture interacting with artificial skin, with respect to surgical suture material and structure, by means of a capstan experiment approach and a contact area model. The results indicated that structure and surface topography of the surgical suture had a pronounced effect on the tribological interactions. The apparent coefficient of friction of vicryl surgical suture was the smallest among the three surgical suture materials. As the sliding velocity increased, or the applied load decreased, the coefficient of friction increased. Furthermore, stick-slip phenomena were observed during the sliding procedure.

Keywords: friction; sliding; surgical suture; artificial skin; capstan experiment

1 Introduction

Surgical sutures are essential for the re-approaching of divided tissues and for the ligation of the cut ends of vessels [1], and play a significant role in wound repair by providing support to healing tissues. The physical properties, handling characteristics, and biological properties affect the basic performance of a surgical suture material [2]. Besides biocompatibility, the ideal surgical suture should (1) be easily pulled through tissues; (2) provide knotting security; (3) allow for easy handling; (4) have predictable tensile strength and performance; and (5) not shrink in tissues. With respect to the ability to be easily pulled through tissues and knotting security, the friction during surgical suture-tissue interactions plays a crucial role. Furthermore, friction generated from the surgical suture relates to the amount of "tissue-drag" and trauma [3].

Researchers have tried to improve the frictional performance of surgical sutures by various methods. Dart and Dart [2] found that the smooth surgical suture surface causes less trauma and is particularly relevant in delicate tissue like the eye. Walling et al. [4] tried to lubricate polyglactin surgical suture by using an antibiotic ointment. It was found that the lubricant could effectively decrease the coefficient of friction and improve the movement of the suture through tissue. Chen et al. [5] treated and modified braided silk surgical suture with an antibacterial agent. Both the static and dynamic friction in surgical suture-to-surgical suture contacts are affected by the antibacterial treatment, reducing friction to about 16% and 33% respectively.

There are many kinds of methods for changing the

* Corresponding author: Xiangqiong ZENG, E-mail: zengxq@sari.ac.cn

composition, structure, and surface of surgical sutures. The number of filaments and the treatment (such as a coating), has a great influence on the surgical suture properties. For instance, according to the number of filaments, surgical sutures can be divided into two kinds: monofilament and multifilament. The two kinds of surgical sutures perform differently in surgery. Monofilament surgical sutures can easily pass through living tissue due to its simple structure, resulting in little frictional resistance. Comparing with multifilament surgical sutures, monofilament surgical sutures contain little pores or interstices, which can effectively reduce the probability of harboring infectious organisms. Multifilament surgical sutures are frequently coated with the benefits of reducing frictional drag and damage to tissue, filling the interstices between fibers, and easing the repositioning of already-tied knots [6]. Three basic structures of surgical sutures, monofilament, multifilament, and coated multifilament, were studied in this paper.

The aim of this study is to understand the tribological behaviour of surgical suture, with respect to surgical suture material and surgical suture structure. Three kinds of suture materials were selected, including nylon, silk, and polygalctin. The paper is organized as follows. Firstly, we described the experiments for evaluating the friction during surgical suture sliding on an artificial skin surface. Secondly, the friction modeling of surgical sutures with different structure sliding on the artificial skin surface was presented. Thirdly, we discussed the effect of surgical suture structure and operational conditions on the tribological interactions between surgical suture and artificial skin. Finally, we drew conclusions and suggested directions for future work.

In order to study the effect of surgical suture structure and operational condition on the surgical suture friction, artificial skin, Silicone Skin L7350 [7], was used to simulate human skin. Because the skin of human and animal has a layered structure with highly changing properties through the layers [8–10], it is hard to control the friction processes at laboratory scale. And Silicone Skin L7350 was used to determinate the skin-surface friction by the Federation Internationale de Football Association (FIFA).

Surgical suture is essentially one kind of fiber used in the medical field. The classical capstan method [11–14], which has been widely used for assessing friction in fibers, was adopted in this study to investigate the frictional performance of surgical sutures. Dry and wet frictional behaviour of the surgical suture and artificial skin interface was studied in this paper, and fetal bovine serum was used in the wet frictional environment in order to simulate the stitching.

The theoretical model of the frictional behaviour of different structures of surgical suture in contact with artificial skin was set up with respect to contact area in this paper. With this modelling effort, the experimental findings could be supported. The theoretical model predicted the contact area as a function of the frictional behaviour of surgical suture.

2 Capstan measurement setup

The capstan measuring approach was used to investigate the frictional behaviour of surgical suture with artificial skin. When a textile material is pulled over a cylindrical body, a frictional force develops between material and cylinder surface due to normal force generated by tensions T_1 and T_2 exerted on the ends. The contact angle sweeps out that portion of circumference over which the contact occurs. The capstan method is designed according the Capstan Eq. (1), which has been the subject of many theoretical and experimental studies in fiber friction.

$$\mu_{\text{app}} = \ln\left(\frac{T_2}{T_1}\right)\frac{1}{\theta_{\text{wrap}}} \tag{1}$$

The apparent coefficient of friction μ_{app} of the surgical suture on the artificial skin was characterized for the suture frictional behaviour, as a function of the applied load T_1 and the tensile force T_2 in the surgical suture ends. The wrapping angle θ was π in this study.

A capstan measurement setup, as illustrated in Fig. 1, was designed by Cornelissen [15, 16], a former colleague of the group. A surgical suture is draped with an angle θ rad over a metal drum (diameter 50.0 mm). The drum is supported by mounts fitted with ball bearings at the ends of the drum on a single aluminium plate. One motor is connected to one end of the drum, which is mounted on the same base plate fitted with ball bearings. There is a motor gearhead

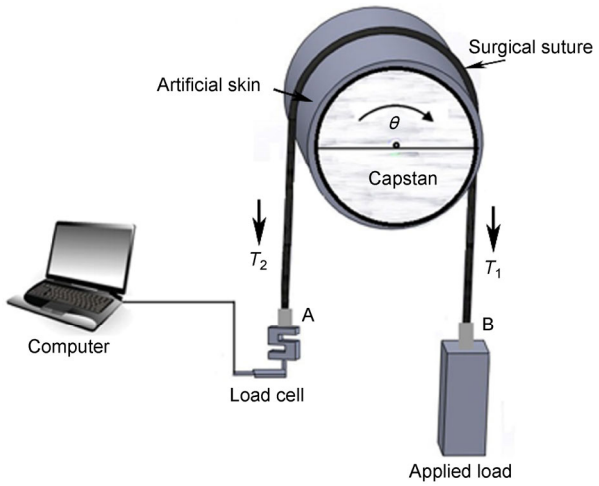

Fig. 1 Capstan experiment for friction characterization of surgical sutures.

between the drum with motor to compensate the misalignments. The force is measured by the single point load cells (range: 0–30 N) equipped with clamps. During the tests, the drum surface is covered with artificial skin by double-side tape. End A of surgical suture is fixed to the load cell; and end B is attached to an applied load.

3 Experiments

3.1 Materials

Nylon (Ningbo Medical Needle Co., Ltd.), a nylon monofilament filament; silk (Yangzhou Fuda Medical Devices CO., LTD), a braided filament; and vicryl (Ethicon, Johnson & Johnson Medical), a synthetic, braided, and absorbable surgical suture made of polyglactin 910, a copolymer of glycolide (90%) and L-lactide (10%), and coated with calcium stearate were used in this study. Silicon Skin L7350 was purchased from Maag Technic AG. Fetal bovine serum (FBS), a physiological fluids, was purchased from Sigma-Aldrich Chemie BV [17].

3.2 Experimental work

The test process was similar to that reported in the previous studies [15, 16] with respect to the frictional behaviour of fibrous tow. The artificial skin was cleaned with acetone and ethanol-impregnated textile wipe, successively before each measurement. During the experiment, the artificial skin was mounted at the cylindrical surface of the metal drum, and fixed with the double-sided foam tape. Then, a surgical suture was draped over the cleaned artificial skin, and surgical suture end A (Fig. 1) was clamped to the load cell measuring force T_2. Subsequently, an applied load T_1 was stably fixed and suspend on the end B of the surgical suture. In each test, the loading duration from the connecting of load to the start of frictional motion is controlled in about 10 s. Tests were carried out in the conditions with or without FBS. FBS was added on the surface of artificial skin at the frequency of one drop per five second. The motor, which was used to drive the drum shaft, was set to work at a rotational frequency, equivalent to a drum surface velocity of 5, 15, or 30 mm/s. The measured loads ranged from 0.1 to 2 N according to the experiments. Each test was repeated for at least three times. The apparent coefficient of friction was calculated by averaging the sampled signal at a steady state approximately 5 s after starting the motor.

3.3 Analysis of the material surface before and after the tribological test

The morphologies of the surgical sutures and the artificial skin before and after experiment were measured by Keyence VK9710 laser confocal microscopy in order to characterize the microstructure of the surgical sutures and the surface topography of the materials. In addition, the surface roughness S_a of all samples was analyzed with a laser confocal microscope VK 9710 from Keyence.

4 Contact model

4.1 Scope of the modeling approach

The model provided an intuitive description of the frictional properties of fibrous surgical suture with respect to the contact area. The friction properties of fibrous surgical suture were considered on the mesoscopic scale, with the aim to afford a relation between the structure of surgical suture and frictional behaviour. The real area of contact was calculated with a Hertzian approach [18].

When surgical suture slides over skin, the lateral

friction force acting at the skin-surgical suture interface is governed by both adhesion and ploughing component, and affected by many factors such as velocity and load.

$$F_{\mathrm{f}} = F_{\mathrm{f,adh}} + F_{\mathrm{f,pl}} \tag{2}$$

The ploughing component $F_{\mathrm{f,pl}}$ of friction in Eq. (2) plays a minor role. Neither any damage nor material transfer to the frictional artificial skin was observed. There was some wear on the surface of artificial skin shown in the Section 5.5. Therefore, for simplicity, it was suggested that the adhesion component at the contact interface between the surgical suture and the artificial skin played the dominant role. The adhesion part of the friction force $F_{\mathrm{f,adh}}$ is determined by the shear strength τ of the materials at the interface and the real contact area A_{r} between them [19]:

$$F_{\mathrm{f,adh}} = \tau A_{\mathrm{r}} \tag{3}$$

The frictional behaviour of fibrous surgical suture on artificial skin related to the real contact area A_{r} in which an interfacial shear strength τ has to be overcome during sliding. The elastic properties and the geometry of the surgical suture impacted the adhesion frictional properties on the contact area. Meanwhile, the modelling procedure with the consideration of the contact area of surgical suture on an artificial skin counterface was shown in Fig. 2.

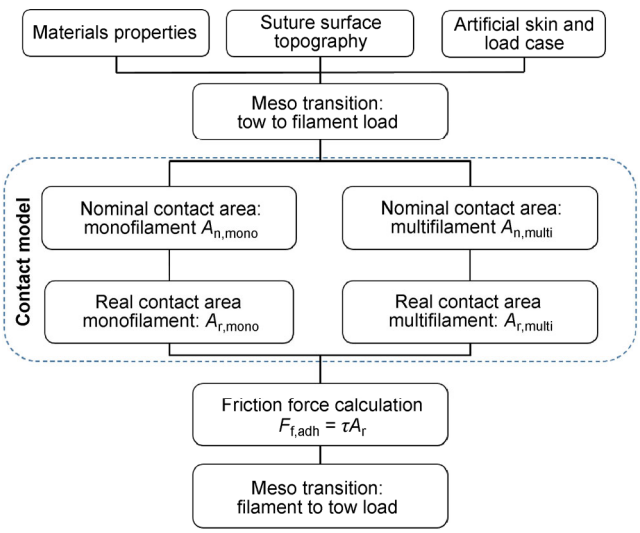

Fig. 2 Contact mechanics modelling procedure of the frictional behaviour of fibrous surgical suture contacting an artificial skin counterface.

4.2 Nominal contact area

The monofilament surgical suture was composed of a cylindrically shaped single fiber. For the multifilament surgical suture, all of the fibers were regularly twisted together to form a cylinder. The multifilament surgical sutures were assumed to be the cylindrically shaped filament without taking the structure and topography of the surgical suture into account. The nominal area of the surgical suture is formed by a line contact as shown in Fig. 3.

The nominal contact area of both monofilament and multifilament surgical suture is calculated by the Hertzian contact (Eq. 4).

$$a_{\mathrm{line}} = \left(\frac{4F_{\mathrm{N,suture}} R_{\mathrm{m}}}{\pi E^{*}} \right)^{1/2} \tag{4}$$

where a_{line} is the half-width of contact and $F_{\mathrm{N,suture}}$ represents the distributed normal load on surgical suture (Fig. 4). R_{m} is the effective radius of curvature, calculated as:

$$R_{\mathrm{m}} = \left(\frac{1}{R_{\mathrm{suture}}} + \frac{1}{R_{\mathrm{flat}}} \right)^{-1} \tag{5}$$

with the surgical suture radius of curvature in transverse direction, the counterface is represented by a flat artificial skin surface, $R_{\mathrm{flat}} = \infty$, thus $R_{\mathrm{m}} = R_{\mathrm{suture}}$.

The equivalent Yong's modulus E^{*} is defined as:

$$E^{*} = \left(\frac{1-v_1^2}{E_1} + \frac{1-v_2^2}{E_2} \right)^{-1} \tag{6}$$

with the fibrous surgical suture properties v_1, E_1, E_2, and v_2 for artificial skin material. From Eq. (4) the nominal contact area $A_{\mathrm{n}} = 2a_{\mathrm{line}}$ per unit filament length (unit: m²/m).

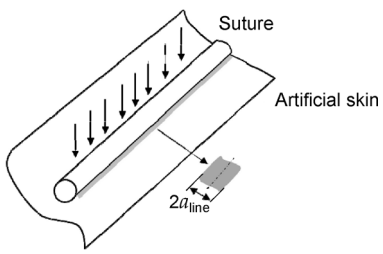

Fig. 3 Schematic drawing of Hertzian contact between a surgical suture and an artificial skin.

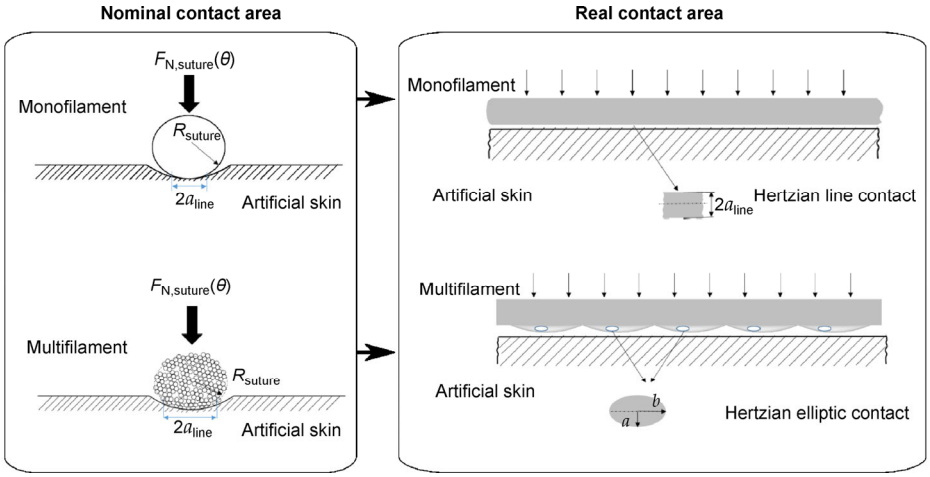

Fig. 4 Nominal and real contact area between a surgical suture and an artificial skin.

4.3 Real contact area

In general, the real contact area for the monofilament surgical suture is close to the nominal contact area as the surface of the monofilament is smoother compared with the multifilament. For multifilament surgical sutures with twisted structure and rough topography, the real contact area is different from the nominal contact area, considering the asperities on the multi-filament surgical sutures. Because the asperities on the multifilament surgical suture is formed by the certain regularly twisted fibers, the asperities could be assumed as several elliptic, as illustrated in Fig. 4. In this case, the real contact area of multifilament $A_{r,multi}$ is the sum of the asperity contact areas. For simplicity, the areas are obtained between a sphere and a cylinder with aligned principal axes by the Hertzian elliptic contact calculation [20]. The elliptic contact area equation has been derived by previous studies [15] as shown in Eq. (7) for a given distributed normal load $F_N(\theta)$, per metre surgical suture length.

$$A_{r,multi} = n_{multi} A_{multi} = n_{multi} \cdot \pi ab \tag{7}$$

where n_{multi} is the number of contacting asperities per meter filament length; a is the semi-minor axis of ellipsoid; b is the semi-major axis of ellipsoid.

5 Results and discussion

5.1 The structure and surface morphology of the materials

In this study, Keyence VK9710 laser confocal microscope was used to detect the surface topography of the surgical suture and the roughness parameters. Roughness is typically considered to be the high-frequency, short-wavelength component of a measured surface. In this research, we used arithmetic mean to describe the surface roughness. We measured the roughness in area (3D, S_a) instead of line (2D, R_a), which can give better information on the surface, for instance including the waviness profile of the filament structure. The laser confocal images of silk, vicryl, and nylon surgical sutures are shown in Fig. 5. The corresponding values of surfaces roughness (S_a) and diameters of the dry and wet surgical sutures are presented in Table 1.

From this figure, it can be seen that, besides nylon (Figs. 5(a, a_1)), both silk (Figs. 5(b, b_1)) and vicryl (Figs. 5(c, c_1)) had many filaments in their structures, and each filament in silk was thinner than that in vicryl. All filaments in vicryl were bound together due to the calcium stearate coating. Therefore, vicryl exhibited better integrity than silk in which all filaments were twisted together.

Table 1 Surface roughness and diameter of the sutures.

Items	Dry		FBS
	S_a (μm)	Diameter (μm)	Diameter (μm)
Nylon	4.25±1.01	74.78±1.23	75.59±0.89
Silk	35.13±5.31	324.81±13.84	416.62±36.34
Vicryl	14.98±2.84	74.44±2.14	87.67±1.29
Artificial skin	0.54±0.23	—	—

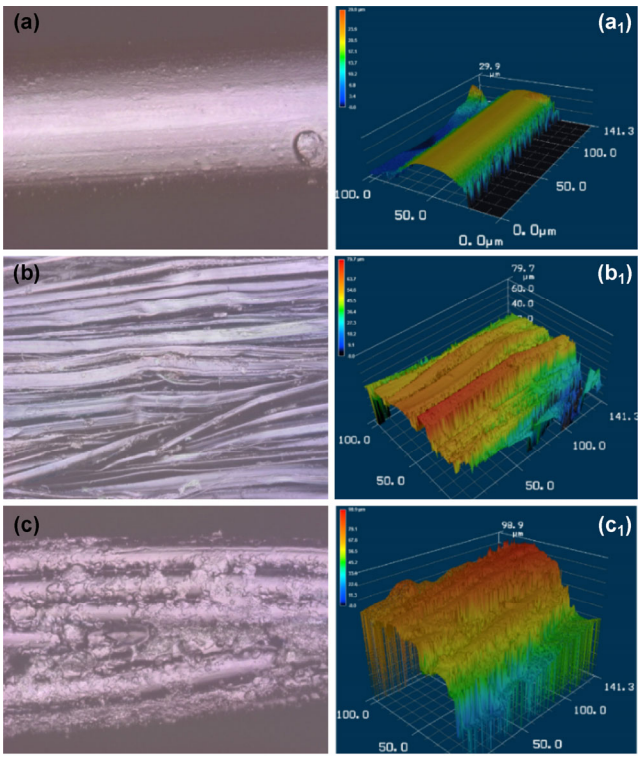

Fig. 5 Laser confocal images of the surgical suture: (a, a_1) Nylon (magnification 100×; pixel represents 0.0675 mm × 0.0675 mm); (b, b_1) silk (magnification 50×; pixel represents 0.135 mm × 0.135 mm), (c, c_1) vicryl (magnification 100×; pixel represents 0.0675 mm × 0.0675 mm).

Nylon was a kind of the monofilament and structure of Nylon is shown in Figs. 5(a, a_1). The model proposed in study is based on the assumption that the surface is smooth. The surface roughness of nylon was 4.25 μm which was the lowest in that of the three kinds of surgical sutures and that of the artificial skin was 0.54 μm as shown in Table 1. The nylon and artificial skin were assumed to be perfectly flat on the mesoscopic scale. The monofilament real contact model was applicable to this case. The real contact area for the monofilament was proportional to the square-root of the distributed normal load according to the Eq. (4).

According to the Eq. (7) mentioned in Section 4.3, the real contact area of multifilament surgical suture was determined by the number of contacting asperities per meter filament length, the semi-minor radius a, and the semi-major radius b. The surface roughness of silk was higher than that of vicryl as a whole, while much higher than that of nylon. According to the theoretical model proposed in this paper, the ratio of A_r/A_n for nylon was close to 1, while that of silk and vicryl was less than 1. Under the same experimental conditions, the contact area of nylon was larger than that of silk and vicryl. Then the friction force of nylon was supposed to be larger than that of the other surgical sutures according to the Eq. (3). Hence, friction forces of the three surgical suture are supposed to be ranked as nylon>silk>vicryl.

5.2 The influence of the applied load on the tribological behaviour

Figure 6 shows the value of apparent coefficient of friction at different applied loads (0.10 to 0.50 N) and the same velocity (15 mm/s) during the sliding between artificial skin and three surgical sutures. The error bars in the graphs indicate the standard deviation of each measurement. Obvious trend can be seen in this figure: the apparent coefficient of friction increased as the applied load decreased. The same trend was also observed by Viju et al. [21, 22] in case of silk-braided surgical sutures. According to the force equilibrium of the surgical suture in an infinitesimal area, the distributed normal load $F_N(\theta)$ at the contact between the fibrous surgical suture and the artificial skin counterface can be calculated as [15]:

$$F_N(\theta) = \frac{T_{\text{suture}}(\theta)}{R_{\text{drum}}} \tag{8}$$

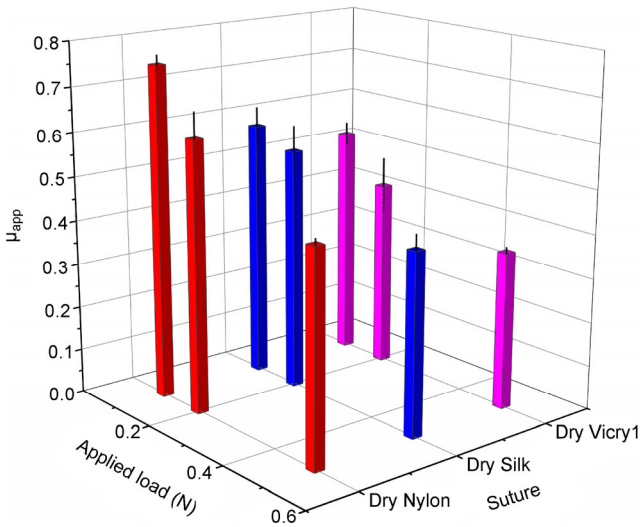

Fig. 6 Apparent coefficient of friction of (a) silk, (b) vicryl, and (c) nylon under different applied load and at 15 mm/s.

The frictional of polymer varies depending on the normal load. However, with the fibrous surgical sutures, the deformation of irregularities is elastic or it may follow an intermediate law. Fibres and polymers do not show a linear relationship between the friction force and the normal load [23]. The surgical suture is one kind of fiber which is a kind of visco-elastic materials. The normal load on the surgical suture was not directly linearly proportional to the friction force. Under higher normal load during elastic deformation, the increased friction force was not linearly proportionally with the normal load increased. During elastic deformation, the real contact area increases less proportionally with the normal load, causing the friction coefficient to decrease under higher load. In this meanwhile, the visco-elastic property of artificial skin was a significant factor to attribute to the decreasing of coefficient of friction with increasing applied load. Young's modulus E of polymer materials depends upon hydrostatic pressure in the contact zone [24]. With increasing of pressure, the modulus of elasticity for silicon is increased many times [25]. There was less deformation on the becoming harder surface of the artificial skin with increasing the Yong's modulus. The shear strength is essentially a creep carried to high deformation. So there was less shear stress when the asperities of the surgical suture slid over at higher applied load.

Another phenomenon seen from Fig. 6 is that, apparent coefficient of friction of the three adopted surgical sutures corresponding to the same normal load were ranked as nylon > silk > vicryl, which could be explained with the real contact models and the surface morphology. According to the real contact area models mentioned in the Section 4, the real contact area of nylon was the largest among the three surgical sutures. For multifilament, the uncoated filaments of silk surgical suture became flat under normal. The semi-minor radius a and the semi-major radius b of silk surgical suture were larger than that of coated vicryl in the same normal load. The contact area between silk surgical suture and artificial skin was larger than that between vicryl surgical suture and artificial skin. The increased real contact area of silk led to the results that apparent coefficient of friction of silk was higher than that of vicryl. This experimental finding verified the prediction mentioned in Section 5.1.

5.3 The influence of velocity on the tribological behaviour

Figure 7 illustrates the variation of apparent coefficient of friction with sliding velocities for silk, vicryl, and nylon subject to 0.20 N applied load. As shown in this figure, with the velocity increasing from 5 to 30 mm/s, apparent coefficient of friction of all the three surgical sutures increased, which was consistent with a similar analysis results trend in Refs. [26–28]. This phenomenon may be contributed to the viscoelastic property of the contacting materials. Textile fibers, being twisted structure and elastic performance, have time-dependent recovery behavior [29]. When load was applied, fibers increased in length, or crept and regularly flowed under the friction force. The disproportionate stress would be transferred to the weaker element of the fiber and cause them to be lengthened. The elastically deformed but unbroken bonds would return to their initial position. The regain at macroscopic dimension was time taken as hysteresis. As there was less time to regain at high velocity comparing with the case at low velocity, the apparent coefficient of friction increased with the increasing of velocity.

5.4 The influence of FBS on the tribological behaviour

Influences of FBS on the friction of three selected surgical sutures after sliding on artificial skin are shown in Fig. 8. It could be seen that, for all the three

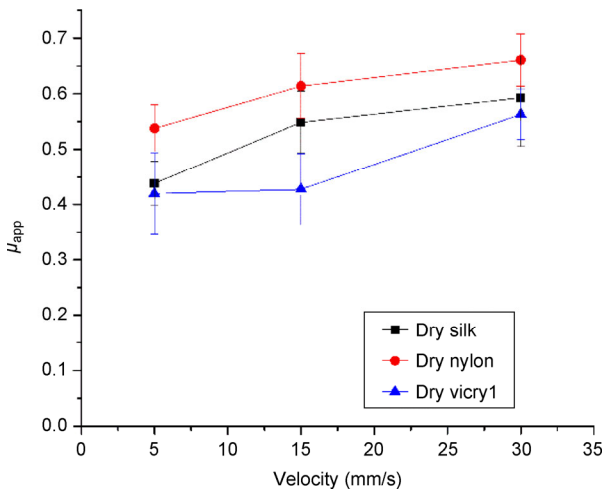

Fig. 7 Apparent coefficient of friction of silk, vicryl, and nylon at various velocity, under 0.20 N applied load.

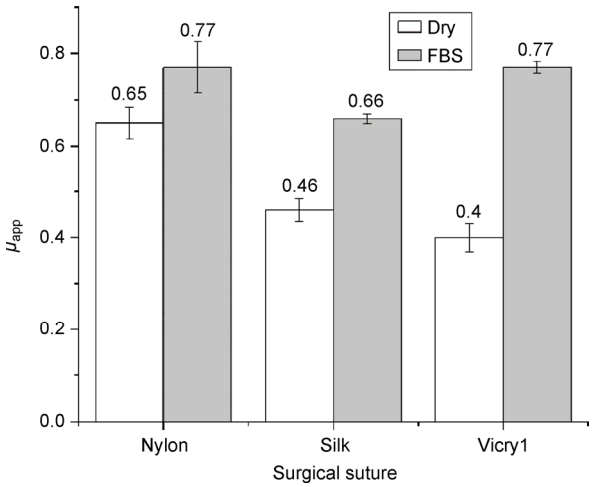

Fig. 8 Apparent coefficient of friction of silk, vicryl, and nylon at dry and the fetal bovine serum conditions under 0.10 N applied load, 15mm/s velocity.

surgical sutures, the apparent coefficient of friction in the condition with FBS was higher than that in dry condition. Reasons for this could be explained from the different contact configurations in the two conditions. There might be a thin FBS film on the contact surface. FBS is a viscous liquid collected from blood fraction. The main components in FBS are proteins and lipids, which can form an adsorbed viscous film on the surface of surgical sutures. The viscous FBS film improves the shear stress, resulting in higher friction coefficient, which was consistent with the findings of literatures [30–32].

The lager differences of apparent coefficient of friction between silk, vicryl, and nylon surgical sutures at dry condition were reduced after adopting FBS due to the absorption of moisture in the surgical suture and the formation of FBS film at the interface. The chemical properties and physical structures of surgical sutures affected their moisture absorption degrees. For instance, silk has hydrophilic group (−OH) that can form hydrogen bonds with water molecules. The twisted structure was in favor of moisture content of surgical suture.

Due to the adsorption of FBS on surgical sutures, the fibers in surgical sutures swelled. The diameters of wet silk, wet vicryl, and wet nylon infiltrated by FBS were measured by using laser confocal microscopy as shown in Table 1. The diameters of wet surgical sutures were all increased compared with the coresponding dry surgical sutures. The increased diameter of silk surgical suture, about 28.26% from 324.81 μm to 416.61 μm, was the highest in the three surgical sutures. The increased diameter ratio of vicryl was about 13.23% and that of nylon was almost no change. The results indicated that surgical suture with multifilament (silk and vicryl) had higher swelling ratio than that with monofilament as shown in Fig. 9. Moreover, coated vicryl exhibited less swelling than uncoated silk due to the better integrity of vicryl as shown in Fig. 2. The resulted increasing ratio in apparent coefficient of friction was: 88.90% for vicryl, 42.70% for silk, and 17.80% for nylon. Although vicryl had less swelling than silk, it demonstrated higher increasing in friction.

This might be due to the fact that the coating film of vicryl prevented adsorption of FBS on its surgical suture, and the coating film was swelled and became adhesive. The adhesion friction force increased due to the moist. Hence, the coating film has a significant effect on the friction when surgical suture slide through artificial skin in the condition with FBS.

5.5 Deformation of the artificial skin

Experimental observations clearly indicated that, after surgical sutures sliding over artificial skin, wear scars were generated on the artificial skin, and the wear scars were more distinct with the increasing of applied load. For low applied load, the shape and size of loaded artificial skin (Figs. 10(b, b')) are similar to that of its original form (Figs. 10(a, a')). Figures 10(c, c') showed the surface morphology and 3D morphology

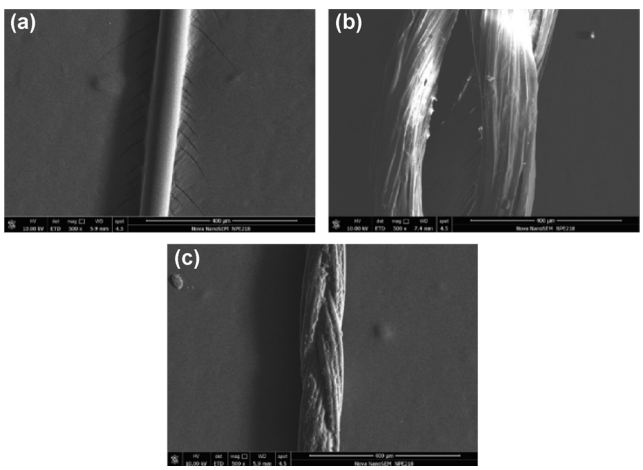

Fig. 9 SEM micrographs of surgical sutures: (a) wet nylon, (b) wet silk, and (c) wet vicryl.

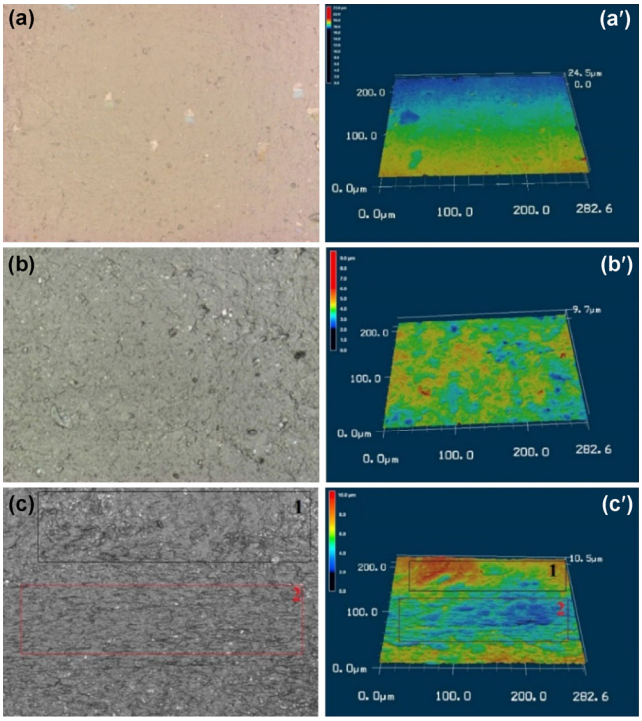

Fig. 10 Surface morphology and 3D morphology of the artificial skin; (a) the surface morphology of the artificial skin; (a') the 3D morphology of the artificial skin; (b) the surface morphology of the artificial skin tests with dry silk at 0.10 N, 5 mm/s; (b') the 3D morphology of the artificial skin tests with dry silk at 0.10 N, 5 mm/s; (c) the surface morphology of the artificial skin tests with dry silk at 2 N, 5 mm/s; (c') the 3D morphology of the artificial skin tests with dry silk at 2 N, 5 mm/s.

of the artificial skin subjected to high applied load. As shown in this figure, the surface roughness (R_a) of unworn area (marked as 1) and wore area (marked as 2) was 0.84 ± 0.06 μm and 1.19 ± 0.08 μm, respectively.

This phenomenon was explained by the influence of applied load on the tribological behavior in Section 5.2. Under high applied load, the rubbing surfaces, which were compressed repeatedly under a certain velocity and applied load, presented roughness. The generation of deformations can be explained by the deformation of the asperities on artificial skins, which could not recover completely after testing. The artificial skin experiences wear under high applied load with the increases of applied load, and the damage of asperities was more serious. Therefore, the wear scars were more distinct. The surface morphologies and 3D morphologies of artificial skin shown in Fig. 10 clearly illustrate this point.

5.6 Stick-slip patterns during sliding

The apparent coefficient of friction profile of the three surgical suture materials subject to 0.10 N applied load with the velocity of 15 mm/s in the conditions with or without FBS are shown in Fig. 11. From this figure, it could be seen that there were friction fluctuations of all the three surgical sutures in the condition without FBS, which was caused by the stick-slip in sliding. Stick-slip is a commonly observed phenomenon in fiber friction tests [12, 33].

Firstly, there was the static friction force (F_s) between surgical suture and artificial skin when there was no relative motion, and the surgical suture moved to a certain limited distant because of the deformation of the surgical suture at F_s. There was the relative motion until the tension force equals or just exceeds F_s. Secondly, the force of the surgical suture had a negative direction of the moving artificial skin because the static friction force (F_s) was less than tangential force which had the same direction with the movement of the artificial skin. At this point, the surgical suture slipped and accelerated back because of an elastic restoring force until the tension dropped to the dynamic friction force (F_d). Due to inertia, surgical suture continued to move back until it came to rest at some value of the force that was less than the dynamic friction force. Then the surgical suture started to move forward until it reached F_d. The friction force once again exceeded the elastic restoring force and the stick-slip cycle began again.

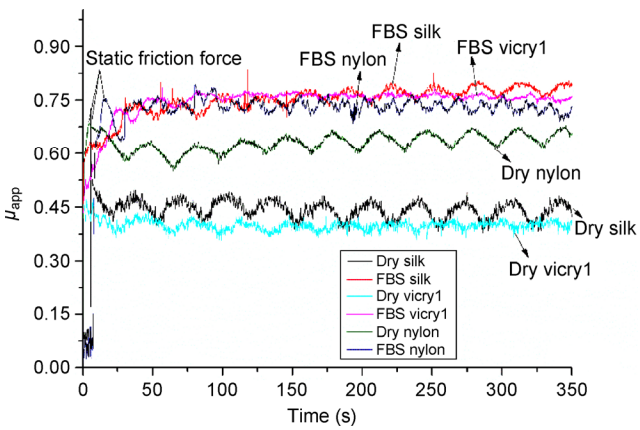

Fig. 11 The friction profile of surgical suture materials under 0.10 N applied load and 15 mm/s velocity.

Because of the difference in stick-slip pattern, the friction fluctuations of the three surgical sutures were rather different from each other (Fig. 11). For all the three surgical sutures, the amplitude of friction fluctuation of vicryl was the smallest, and the friction profile of vicryl was the smoothest in each period. There was the following possible reason for this trend. The relative velocity between surgical suture and artificial skin was different at the process of stick-slip move, and the dwell time became less at the high relative velocity. Studies indicated that contact duration or dwell time can markedly influence the level of rubber adhesion and friction [34]. When the artificial skin regularly slided, the relative velocity was changed as the tensile change.

The amplitude of friction fluctuation was significantly decreased due to the existing of FBS for the three surgical sutures, as shown in Fig. 11. This means that when surgical suture slided through artificial skin, the different between static friction force and dynamic friction force in wet condition was less than that in dry condition. When FBS was used in the experiment, FBS replaced the air and filled into the space between surgical suture and artificial skin. The three surgical sutures should overcome the same the force caused by the viscous FBS. So the coefficient of friction of the surgical sutures was similar at the present of FBS.

The less stick-slip phenomenon and amplitude of friction fluctuation occurred, the better the stitching was. It was supposed that the larger fluctuations caused greater damage to the skin. Therefore, for the three surgical sutures, the existing of FBS, which decreased the amplitude of friction fluctuation, was supposed to be benefit for the stitching.

6 Conclusion

The monofilament and multifilament contact models provided a physically understanding of the frictional behaviour between surgical suture and an artificial skin counterface. With the proposed model the experimentally observed frictional behaviour of fibrous surgical suture was explained with theoretical support.

A classical capstan method developed for the tribological study of fibers, was adopted to investigate the tribological interaction between surgical sutures and artificial skin in this study. The frictional behaviour of surgical suture was investigated by means of a quantitative comparison of three basic structure of sutures and experimental conditions. The structure and surface topography of the surgical suture was the main parameter affecting the frictional behaviour of surgical-artificial skin contact. The apparent coefficient of friction of vicryl, which was multifilament structure and coated with calcium stearate, was the smallest among the three surgical suture materials. The coated multifilament structure of the surgical suture, reduced the friction during sliding, was supposed to be benefit for the stitching. This had the certain reference significance for the future study about surgical suture development. As the surgical suture sliding velocity increased, or the applied load decreased, the apparent coefficient of friction increased. It was found that the apparent coefficient of friction increased from 0.40 to 0.77 as the fetal bovine serum added during the sliding between artificial skin and vicryl.

The stick-slip phenomena were observed in the tests with and without fetal bovine serum. The amplitude of friction fluctuation was significantly decreased due to the existing of FBS for the three surgical sutures. The existing of FBS can decrease the amplitude of friction fluctuation, but it also increased the coefficient of friction.

Acknowledgement

The authors are grateful to Marie Curie CIG (No. PCIG10-GA-2011-303922), the Shanghai Municipal "Science and Technology Innovation Action Plan" International Cooperation Project (No. 15540723600) for the financial support.

References

[1] Thacker J G, Rodeheaver G, Moore J W, Kauzlarlch J J, Kurtz L, Edgerton M T, Edlich R F. Mechanical performance of surgical sutures. *Am J Surg* **130**: 374–380 (1975)

[2] Dart A J, Dart C M. Suture material: Conventional and stimuli responsive. *Comprehensive Biomaterials* **6**: 573–587 (2011)

[3] Apt L, Henrick A. "Tissue-drag" with polyglycolic acid (Dexon) and polyglactin 910 (Vicryl) sutures in strabismus surgery. *J Pediatr Ophthalmol* **13**: 360–364 (1976)

[4] Walling H W, Christensen D R, Arpey C J, Whitaker D C. Surgical pearl: Lubrication of polyglactin suture with antibiotic ointment. *J Am Acad Dermatol* **52**(1): 136–137 (2005)

[5] Chen X, Hou D, Tang X, Wang L. Quantitative physical and handling characteristics of novel antibacterial braided silk suture materials. *J Mech Behav Biomed Mater* **50**: 160–170 (2015)

[6] El Mogahzy Y E. Development of textile fiber products for medical and protection applications. *Engineering Textiles* **2009**: 475–525 (2009)

[7] Van Der Heide E, Lossie C M, Van Bommel K J C, Reinders S A F, Lenting H B M. Experimental investigation of a polymer coating in sliding contact with skin-equivalent silicone rubber in an aqueous environment. *Tribol Trans* **53**: 842–847 (2010)

[8] Van Der Heide E, Zeng X, Masen M A. Skin tribology: Science friction? *Friction* **1**: 130–142 (2013)

[9] Morales-Hurtado M, Zeng X, Gonzalez-Rodriguez P, Ten Elshof J E, van der Heide E. A new water absorbable mechanical Epidermal skin equivalent: The combination of hydrophobic PDMS and hydrophilic PVA hydrogel. *J Mech Behav Biomed Mater* **46**: 305–317 (2015)

[10] van Kuilenburg J, Masen M A, van der Heide E.. Contact modelling of human skin: What value to use for the modulus of elasticity? *Proc IMechE, Part J: J Eng Tribol* **227**: 349–361 (2012)

[11] Robins M M, Rennell R W, Arnell R D. The friction of polyester textile fibres. *J Phys D: Appl Phys* **17**: 1349–1360 (1984)

[12] Tu C-F, For T. A study of fiber-capstan friction. 2. Stick–slip phenomena. *Tribol Int* **37**: 711–719 (2004)

[13] Gao X, Wang L, Hao X. An improved Capstan equation including power-law friction and bending rigidity for high performance yarn. *Mechanism and Machine Theory* **90**: 84–94 (2015)

[14] Tu C-F, For T. A study of fiber-capstan friction. 1. Stribeck curves. *Tribol Int* **37**: 701–710 (2004)

[15] Cornelissen B, de Rooij M B, Rietman B, Akkerman R. Frictional behaviour of high performance fibrous tows: A contact mechanics model of tow–Metal friction. *Wear* **305**: 78–88 (2013)

[16] Cornelissen B, Rietman B, Akkerman R. Frictional behaviour of high performance fibrous tows: Friction experiments. *Compos Part A: Appl Sci Manuf* **44**: 95–104 (2013)

[17] Amaral M, Abreu C, Oliveira F, Gomes J, Silva R. Tribological characterization of NCD in physiological fluids. *Diamond and Related Materials* **17**: 848–852 (2008)

[18] Johnson K L, Greenwood J A. An adhesion map for the contact of elastic spheres. *J Colloid Interface Sci* **192**: 326–333 (1997)

[19] Roselman I C, Tabor D. The friction and wear of individual carbon fibres. *J Phys D: Appl Phys* **10**: 1181–1194 (1977)

[20] Johnson K L. *Contact Mechanics*. Cambridge University Press, 1987.

[21] Viju S, Thilagavathi G. Effect of chitosan coating on the characteristics of silk-braided sutures. *Journal of Industrial Textiles* **42**: 256–268 (2012)

[22] Hendrikson W J, Zeng X, Rouwkema J, van Blitterswijk C A, van der Heide E, Moroni L. Biological and Tribological assessment of poly (ethylene oxide terephthalate)/poly (butylene terephthalate), polycaprolactone, and poly (L\DL) lactic acid plotted scaffolds for skeletal tissue regeneration. *Adv Healthc Mater* **5**(2): 232–243 (2016)

[23] Yuksekkaya M E. More about fibre friction and its measurements. *Textile Progress* **41**: 141–193 (2009)

[24] Ferry J D. Viscoelastic properties of polymers polymer solutions. *J Res Natl Bur Stand* **41**(1): 53–62 (1948)

[25] Boiko A V, Kulik V M, Seoudi B M, Chun H H, Lee I. Measurement method of complex viscoelastic material properties. *International Journal of Solids and Structures* **47**: 374–382 (2010)

[26] Roth F L, Driscoll R L, Holt W L. Friction properties of rubber. *Joumal of Research of the National Bureau of Standards* **28**: 440–461 (1942)

[27] Grosch K A. The relation between the frciton and visco-elastic properties of rubber. *Proceedings of the Royal Society A: Mathematical, Physical and Engineering Sciences* **274**(1356): 21–39 (1963)

[28] Howell H G, Mieszkis K W, Tabor D. *Friction in Textiles*. London (UK): Butterworths Scientific Publications, 1959.

[29] Gupta B. Textile fiber morphology, structure and properties in relation to friction. *Friction in Textile Materials* **2008**: 3–36 (2008)

[30] Amaral M, Abreu C S, Oliveira F J, Gomes J R, Silva R F. Biotribological performance of NCD coated Si_3N_4-bioglass composites. *Diamond and Related Materials* **16**: 790–795 (2007)

[31] Briscoe B. The role of adhesion in the friction, wear and lubrication of polymers. *Adhesion* **5**: 49–80 (1981)
[32] Hansen W W, Tabor D. Role of hydrodynamic lubrication in the friction of fibers and yarns. *J Appl Phys* **27**(12): 1558–1559 (1956)
[33] Griesser H J, Chatelier R C, Martin C, Vasic Z R, Gengenbach T R, Jessup G. Elimination of stick-slip of elastomeric sutures by radiofrequency glow discharge deposited coatings. *J Biomed Mater Res* **53**(3): 235–243 (2000)
[34] Roberts A, Thomas A. The adhesion and friction of smooth rubber surfaces. *Wear* **33**: 45–64 (1975)

Gangqiang ZHANG. He received his master degree in chemistry and chemical engineering in 2013 from Qingdao University, Qingdao, China. Now, he is a Ph.D. student in the Key Laboratory for Thin Film and Microfabrication of the Ministry of Education, School of Chemistry and Chemical Engineering, Shanghai Jiao Tong University, China. Meanwhile, he is also a Ph.D. student in mechanical engineering at University of Twente, Enschede, the Netherlands. His research interests include biotribology of medical material and development of lubricants.

Xiangqiong ZENG. She received her MSc. degree in applied chemistry and Ph.D. degree in material science from Shanghai Jiao Tong University, in 2003 and 2006 respectively. After then, she worked as a staff scientist in Johnson & Johnson on Skin Care Technology for 5 years, and then as a Tenure Track Assistant Professor in University of Twente, the Netherlands, on skin and human tissue tribology for 5 years. She joined Shanghai Advanced Research Institute, Chinese Academy of Sciences from November 2015 and her current position is a professor at the Advanced Lubricating Materials Laboratory. Her research areas cover biotribology and hydration lubrication, including active control of friction and wear by surface and interface design of skin contacting materials and medical devices, by test methodology development with the design of instrument and bio-inspired human tissue model, and by additive and emulsion development for hydration lubrication.